Available online at www.sciencedirect.com
SCIENCE DIRECT
Solid State Communications 137 (2006) 288–291
solid state communications
www.elsevier.com/locate/ssc

# Giant electroresistance and nonlinear conduction in electron-doped $Ca_{0.9}Ce_{0.1}MnO_3$

W.J. Lu *, Y.P. Sun, B.C. Zhao, X.B. Zhu, W.H. Song

*Key Laboratory of Materials Physics, Institute of Solid State Physics, Chinese Academy of Sciences, Hefei 230031, People's Republic of China*

Received 1 September 2005; received in revised form 29 November 2005; accepted 5 December 2005 by T.T.M. Palstra
Available online 27 December 2005

**Abstract**

We report a large resistance drop induced by Dc electrical currents in charge-ordered $Ca_{0.9}Ce_{0.1}MnO_3$. A giant electroresistance (ER) of ~90% at 100 mA current below charge ordering (CO) transition temperature ($T_{CO}$) is found. Nonlinear conduction, which starts above a threshold current, gives rise to a region of negative differential resistance (NDR). The nonlinear conduction cannot be explained by homogeneous Joule heating of the sample. The origin of these phenomena is discussed in view of current induced collapse of CO state associated with phase-separation mechanism. This work can be useful for the potential applications of ER such as nonvolatile memory elements.


*PACS:* 75.47.Lx; 72.60.+g; 73.50.Fq; 64.75.+g

*Keywords:* A. Manganites; D. Giant electroresistance; D. Nonlinear conduction

## 1. Introduction

The phenomena of colossal magnetoresistance (CMR) in mixed-valent manganites have attracted considerable attention in recent years due to the related physics and potential applications [1–3]. One particular interest is the study of the behavior of the ordered state in these compounds. Charge ordering (CO) is a common characteristic of transition metal oxides with perovskite structure. In CMR manganites, the formation of a $Mn^{3+}$:$Mn^{4+}$ ordered phase is the most obvious manifestation of the $e_g$ electrons localization. The competition between the CO insulating state and the charge delocalized (CD) state which presents a metallic conductivity, is of a great attention [4,5]. Moreover, many experiments have shown that the CO state is unstable under a variety of external perturbations including magnetic field [6], electric field [7–9], and optical radiation [10]. Application of an electric field (current) also gives rise to nonlinear conduction. Many of these nonlinear effects have often been attributed to depinning transitions or to melting of CO state. In addition, Palanisami et al. [11] suggested that the nonuniform Joule heating should be considered as a possible cause or contributor to the formation of nonlinear effects under strong current bias.

Recently, a quite large resistance change by an external electric field, i.e. giant electroresistance (ER) was observed in $Pr_{1-x}Ca_xMnO_3$ and triggered a surge of research on its potential for practical applications such as nonvolatile memory elements [12,13]. The system behaves in such a way that the bias current may generate metallic path giving rise to resistivity drop. On the other hand, a giant ER near the $T_c$ in thin film of ferromagnetic $La_{0.7}Ca_{0.3}MnO_3$ and $Pr_{0.8}Ca_{0.2}MnO_3$ has also been reported [14,18]. Current induced metastable resistive states have been also observed in manganites [15,16]. We notice that the majority of studies of ER effects were performed mainly on the hole-doped (p-type) manganites. In the present paper, we study the current-induced effect on the electron-doped (n-type) manganite $Ca_{0.9}Ce_{0.1}MnO_3$. Such a study in n-type manganite may be useful for the future applications of ER in p–n junction, combined with the studies in p-type manganites.

Zeng et al. [17] have reported that $Ca_{0.9}Ce_{0.1}MnO_3$ undergoes a CO transition at around $T_{CO}$ ($T_{CO}=170$ K), at which an antiferromagnetic (AFM) ordering appears. In this paper, we study the giant ER and the nonlinear conduction in this sample. A negative differential resistance (NDR) is observed when the bias current $I$ exceeds a current threshold ($I_{th}$). Under an applied magnetic filed of 8 T, the $I_{th}$ value has no obvious change. The typical current-switching effect has

* Corresponding author. Tel.: +86 551 5592757; fax: +86 551 5591434.
*E-mail addresses:* wjlu@issp.ac.cn (W.J. Lu), ypsun@issp.ac.cn (Y.P. Sun).

0038-1098/$ - see front matter © 2005 Elsevier Ltd. All rights reserved.
doi:10.1016/j.ssc.2005.12.005

also been observed. These phenomena have been interpreted in terms of current induced collapse of CO state associated with phase-separation mechanism.

## 2. Experimental details

Polycrystalline $Ca_{0.9}Ce_{0.1}MnO_3$ sample was synthesized by the standard solid-state reaction. Stoichiometric precursor powders $CaCO_3$, $CeO_2$, and $MnO_2$ were mixed and ground, then fired in air several times at 1050, 1200, and 1300 °C for 24 h with intermediate grinding. After the final grinding, the powder was pressed into small pellets, sintered at 1350 °C for 24 h and slow-cooled to room temperature.

The room temperature X-ray diffraction (XRD) measurement was taken by Philips X'pert PRO X-ray diffractometer with Cu $K_\alpha$ radiation. The resistivity $\rho$ was measured by means of a quantum design physical property measurements system (PPMS) using the standard four-probe method. The measurements of voltage–current ($V$–$I$) were taken with current biasing. The Dc currents in the PPMS are selected in our measurements.

## 3. Results and discussion

The room temperature XRD results show that the sample is single phase with monoclinic structure ($P2_1/m$ space group). The measurements of electrical transport (see the inset of Fig. 1) indicate the CO state appears below $T_{CO}$ ($\approx$170 K), which has been reported in recent paper [17]. Fig. 1 shows the temperature dependence of resistivity of $Ca_{0.9}Ce_{0.1}MnO_3$ under different Dc currents. Fig. 1 clearly shows that the resistivity decreases with increasing the applied currents ($I$=0.01–100 mA). For higher currents (50 and 100 mA), the resistivity is strongly depressed especially at low temperatures. Under 100 mA current, the resistivity drops abruptly by over two orders of magnitude. The observed behavior is rather similar to that of $Pr_{0.63}Ca_{0.37}MnO_3$ crystal, for which the electrical current triggers the collapse of the low-temperature electrically insulating CO state to a ferromagnetic metal (FMM) state [8].

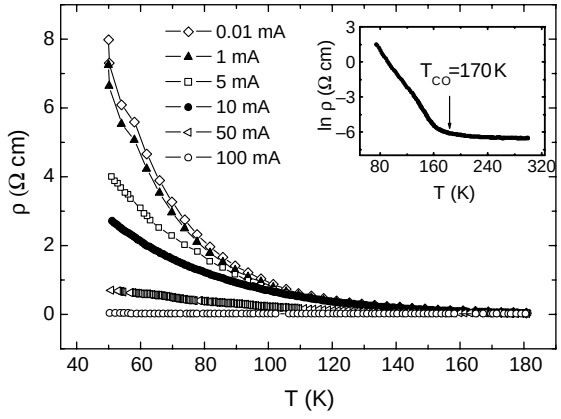


Fig. 1. Temperature dependence of resistivity $\rho$ under different measuring currents (0.01–100 mA). The inset shows the ln $\rho(T)$ curve under measuring current 0.01 mA. $T_{CO}$ is the charge ordering temperature.

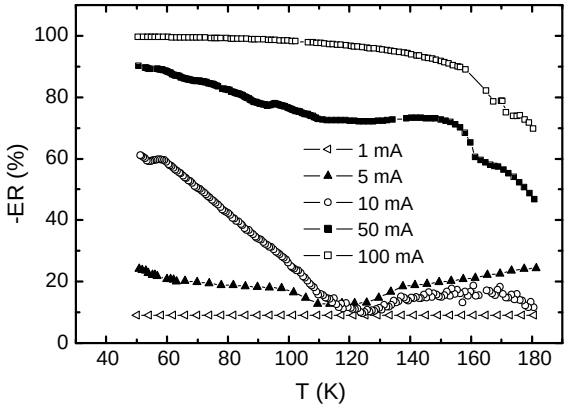


Fig. 2. Temperature dependence of electroresistance (ER) with different applied currents. The ER is defined as $[\rho(I)-\rho(0.01\ \text{mA})]/\rho(0.01\ \text{mA})$.

Fig. 2 describes the temperature dependence of ER under different currents. The ER, defined as $[\rho(I)-\rho(0.01\ \text{mA})]/\rho(0.01\ \text{mA})$, is negative because the current reduces the resistance. For $I$=1 mA, the ER is about 10% and almost temperature-independent. The ER increases abruptly as measuring current exceeds 10 mA. For the highest current (100 mA), the ER is near 99.5% at 50 K. The giant ER decreases with increasing temperature. At around $T_{CO}$, the ER drops abruptly with increasing temperature. Although the heating can have some influence on the value of $\rho$ at the highest measuring current, the simple Joule heating cannot account for the observed giant ER, considering such a large change of resistivity. The giant ER effects in charge-ordered samples can be explained by the model that current injects into highly conducting filamentary paths [7,19]. The bias current may generate metallic path and break the CO state giving rise to resistivity drop.

The $V$–$I$ characteristics at different temperatures under zero magnetic field are shown in Fig. 3. Above $T_{CO}$, an Ohmic conduction is observed in the whole current range. The $V$–$I$ characteristics for temperatures (200 and 300 K) are displayed in the inset of Fig. 3. Below $T_{CO}$, nonlinear conduction was observed. As bias current exceeds a threshold value $I_{th}$, the behavior of NDR ($dV/dI<0$) appears. For instance, at 50 K an

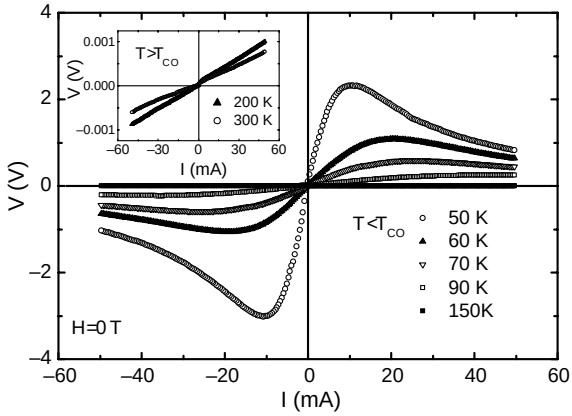


Fig. 3. $V$–$I$ characteristics under zero magnetic field for temperatures below $T_{CO}$. The inset shows the $V$–$I$ curves for temperatures above $T_{CO}$.

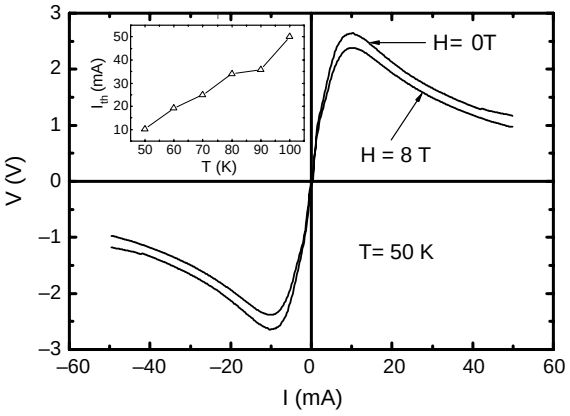


Fig. 4. *V–I* characteristics under zero and 8 T magnetic field at 50 K. The inset shows the temperature dependence of threshold current $I_{th}$ determined from *V–I* curves.

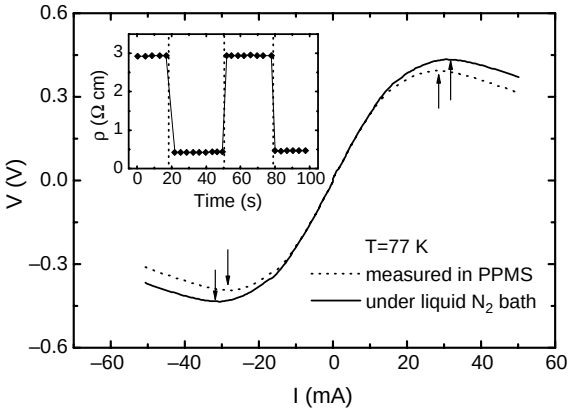


Fig. 5. *V–I* characteristics performed under liquid $N_2$ bath (solid line) and in the PPMS (dotted line). The arrows indicate the threshold current $I_{th}$. The inset shows the time dependence of resistivity measured using the alternately varied currents 0.01 and 50 mA under liquid $N_2$ bath. The times, at which the applied current is changed, are marked with dotted lines.

increase of the current breaks Ohmic relation at 10 mA and causes a decrease in voltage. A symmetric *V–I* curve indicates the reproducibility of the *V–I* characteristics. In the region of NDR, it is found that *V–I* curves follow the relationship of $V\text{–}I^{-n}$, where $0<n<1$, which has been observed in charge-ordered $Pr_{0.63}Ca_{0.37}MnO_3$ [8]. The temperature dependence of $I_{th}$ are shown in the inset of Fig. 4. The $I_{th}$ is 10 mA at 50 K up to 50 mA at 100 K. The threshold current $I_{th}$ increases with increasing temperature, which is consistent with that observed in $Pr_{0.63}Ca_{0.37}MnO_3$ sample by other authors [8,20]. At lower temperatures, the smaller $I_{th}$ may imply that the CO state is more instable due to the competition between the CO and CD phases.

We have also measured *V–I* curves at different temperatures under applied magnetic fields of 3, 5, and 8 T. The experimental results indicate that the *V–I* characteristics are not strongly modified under magnetic field. As an example, Fig. 4 shows measurements at 50 K under zero and 8 T magnetic field. It can be observed that the NDR region sets in for rather close values of the current threshold. The results suggest that for a sufficient bias current, a conduction path is opened and the magnetic field does not trigger or limit this phenomenon. If it is assumed that a magnetic-field-induced transformation of AFM CO insulating state into FMM appears, the disappearance of the NDR upon application of magnetic field should be observed like in the charge-ordered $Pr_{1-x}Ca_xMnO_3$ ($x\approx0.3$) system [7,8]. However, the NDR effect in $Ca_{0.9}Ce_{0.1}MnO_3$ is hardly affected by the 8 T magnetic field. The facts shows that the CO state in $Ca_{0.9}Ce_{0.1}MnO_3$ may be much stable and it needs higher magnetic field to melt the CO state.

In order to minimize the heating effect, we put the probe into liquid $N_2$ instead of the cryostat, as in other authors design [21]. In Fig. 5, the *V–I* characteristics performed under liquid $N_2$ bath are compared with those performed in the PPMS. It is found that the nonlinear conduction and NDR are still observed in the *V–I* characteristics performed under liquid $N_2$ bath, which cannot possibly be explained by simple Joule heating. Although the heating effect is not a major contribution to the nonlinear conduction and NDR, the Joule heating is still be probably considered to have some influence on the *V–I* characteristics performed in the PPMS. In fact, one can see that the *V–I* curves performed under liquid $N_2$ bath and in the PPMS do not overlap in the whole measuring current range, especially for the larger currents ($I>10$ mA). For a constant *I*, the measured value of *V* in the PPMS is smaller than that under liquid $N_2$ bath. This difference of the values of *V* should be attributed to the heating effect. Unlike the measurements under the liquid $N_2$ bath where the heating effect is almost eliminated, the measurements in the PPMS can be affected by the heating effect in a certain extent, especially for the larger measuring currents. The resistance of the sample decreases due to the Joule heating, consequently the value of *V* in the PPMS is smaller than that under liquid $N_2$ bath. In addition, the heating effect can have little influence on the value of the threshold current $I_{th}$. The values of the threshold current $I_{th}$ measured in the PPMS and under liquid $N_2$ bath are 28 and 31 mA, respectively.

At the liquid-nitrogen temperature (77 K), we have also measured the resistance by the alternately varied currents (0.01–50 mA). The time dependence of resistivity is shown in the inset of Fig. 5. Initially, the resistivity is about 2.8 Ω cm as the 0.01 mA current is applied. Then, the current rapidly changes to 50 mA and accordingly the resistivity drops to around 0.5 Ω cm. The switch between the higher-resistivity and lower-resistivity states is the typical current-switching effect. In addition, there is no hysteresis in the current-switching, which indicates the measurements should be less affected by the heating effect. The change of the resistivity is much larger, which is reversible and nonvolatile. Such a behavior can be useful for the potential applications in nonvolatile memory elements [22]. The ON- and OFF- states could be written to the elements by applying appropriate voltages (currents) to the gate. The current-switching phenomena reported here may involve dielectric breakdown of the charge-ordered state, in which the charge carriers are initially localized. The dielectric breakdown of such states should immediately lead to the appearance of a metallic state

accompanied by a large number of mobile charge carriers, and hence is intrinsically different from conventional semiconductors or band insulators [7].

The observed nonlinear conduction, and more particularly the NDR, can be explained using the phase-separation (PS) scenario [23], which consists of a fine mixture of the two competing ground states, the FMM state and the charge/orbital-ordered insulator one. The resistivity of the PS system does not depend solely on the ratio of the volumes of coexisting phases, but also in a crucial way depends on the distribution of the conductive domains and their size and shape. The strong current will inject to the PS system and enforce changes of the topology of the phase coexistence. For $I > I_{th}$, metallic filaments open up, which will provide parallel paths of conduction. Nonlinear conduction can also occur due to depinning of CO domains above a threshold applied field as has been reported earlier [24]. Other mechanisms of current-induced effect such as the charge density wave (CDW) scenario has also been proposed by Mercone et al. [20]. In this scenario, if an electric field strong enough to overcome the pinning energy is applied, the CDW can be depinned and carries a current. Although a theoretical understanding of the mechanisms in current-induced effects is still incomplete, the PS scenario is commonly adopted as a main ingredient.

## 4. Conclusion

In summary, we have carried out a systematic investigation of the nonlinear transport in the electron-doped $Ca_{0.9}Ce_{0.1}MnO_3$. A giant ER is observed, which is not interpreted by the simple Joule heat. We find that a NDR region shows up below $T_{CO}$, as applied current exceeds a threshold value. These phenomena have been explained in terms of PS scenario. The current-switching effect is useful for the potential applications in nonvolatile memory elements.

## Acknowledgements

This work was supported by the National Key Research under Contract No. 001CB610604, and the National Nature Science Foundation of China under Contract Nos. 10374033 and 10474100, and the Fundamental Bureau, Chinese Academy of Sciences.

## References

[1] S. Jin, T.H. Tiefel, M. McCormack, R.A. Fastnacht, R. Ramesh, L.H. Chen, Science 264 (1994) 413.
[2] Y. Tokura, Y. Tomioka, H. Kuwahara, A. Asamitsu, Y. Moritomo, M. Kasai, J. Appl. Phys. 79 (1996) 5288.
[3] Y. Tokura, Colossal Magnetoresistance Oxides, Gordon and Breach, New York, 2000.
[4] P. Schiffer, A.P. Ramirez, W. Bao, S.-W. Cheong, Phys. Rev. Lett. 75 (1995) 3336.
[5] G. Varelogiannis, Phys. Rev. Lett. 85 (2000) 4172.
[6] H. Kuwahara, Y. Tomioka, A. Asamitsu, Y. Moritomo, Y. Tokura, Science 270 (1995) 961.
[7] A. Asamitsu, Y. Tomioka, H. Kuwahara, Y. Tokura, Nature 388 (1997) 50.
[8] A. Guha, A.K. Raychaudhuri, A.R. Raju, C.N.R. Rao, Phys. Rev. B 62 (2000) 5320.
[9] P. Padhan, W. Prellier, Ch. Simon, R.C. Budhani, Phys. Rev. B 70 (2004) 134403.
[10] M. Fiebig, K. Miyano, Y. Tomiyoka, Y. Tokura, Science 280 (1998) 1925.
[11] A. Palanisami, M.B. Weissman, N.D. Mathur, Phys. Rev. B 71 (2005) 094419.
[12] S.Q. Liu, N.J. Wu, A. Ignatiev, Appl. Phys. Lett. 76 (2000) 2749.
[13] A. Baikalov, Y.Q. Wang, B. Shen, B. Lorenz, S. Tsui, Y.Y. Sun, Y.Y. Xue, C.W. Chu, Appl. Phys. Lett. 83 (2003) 957.
[14] J. Gao, S.Q. Shen, T.K. Li, J.R. Sun, Appl. Phys. Lett. 82 (2003) 4732.
[15] V. Markovich, G. Jung, Y. Yuzhelevski, G. Gorodetsky, A. Szewczyk, M. Gutowska, D.A. Shulyatev, Ya.M. Mukovskii, Phys. Rev. B 70 (2004) 064414.
[16] J. Gao, F.X. Hu, Appl. Phys. Lett. 86 (2005) 092504.
[17] Z. Zeng, M. Greenblatt, M. Croft, Phys. Rev. B 63 (2001) 224410.
[18] S. Mercone, A. Wahl, Ch. Simon, C. Martin, Phys. Rev. B 65 (2002) 214428.
[19] C.N.R. Rao, A.R. Raju, V. Ponnambalam, S. Parashar, N. Kumar, Phys. Rev. B 61 (2000) 594.
[20] S. Mercone, A. Wahl, A. Pautrat, M. Pollet, Ch. Simon, J. Magn. Magn. Mater. 272 (2004) 388.
[21] Y.G. Zhao, Y.H. Wang, G.M. Zhang, B. Zhang, X.P. Zhang, C.X. Yang, P.L. Lang, M.H. Zhu, P.C. Guan, Appl. Phys. Lett. 86 (2005) 122502.
[22] K.N. Narayanan Unni, R. de Bettignies, S. Dabos-Seignon, J.-M. Nunzi, Appl. Phys. Lett. 85 (2004) 1823.
[23] A. Moreo, S. Yunoki, E. Dagotto, Science 283 (1999) 2034.
[24] A. Guha, A. Ghosh, A.K. Raychaudhuri, S. Parashar, A.R. Raju, C.N.R. Rao, Appl. Phys. Lett. 75 (1999) 3381.